Acta Geod Geophys (2017) 52:331–343
DOI 10.1007/s40328-016-0172-6

ORIGINAL STUDY

Numerical evolution of the asymmetry in the compositionally inhomogeneous lower mantle driven by Earth's rotation

Tamás Bozóki[1] · **Mátyás Herein**[1] · **Attila Galsa**[1]

Received: 5 January 2016 / Accepted: 4 April 2016 / Published online: 12 April 2016
© Akadémiai Kiadó 2016

Abstract Numerical model calculations have been carried out to study the effect of the centrifugal force on the compositionally dense material accumulated in the lowermost mantle. The deformation of an initial dense layer encircling the core was investigated systematically as a function of the density difference between the lower dense and the overlaying mantle, β and the angular velocity of the planet, Ω in a two-dimensional cylindrical shell domain. It was established that increasing β does not influence the magnitude of the deformation of the dense layer but decreases the velocity of the deformation. The relaxation time of the deformation is inversely proportional to β similarly to post-glacial rebound. On the other hand, increasing Ω enhances the magnitude of the deformation but does not affect the deformation relaxation time. The magnitude of the deformation is approximately proportional to Ω^2. It was pointed out that for the present-day mantle parameters, $\beta = 2$–4 % and $\Omega = 7.3 \times 10^{-5}$ 1/s the equatorial elevation of the dense layer is about 2 km which more than two orders of magnitude less than the height of the seismically observed large low shear velocity provinces beneath Africa and Pacific. During the Earth's history when the rotation of our planet was faster the influence of the centrifugal force was much more significant and the equatorial elevation of the dense layer might have reached even 100 km.

Keywords Mantle convection · Earth's rotation · Large low shear velocity provinces · Numerical modelling

1 Introduction

The rotation of the Earth plays a crucial role in numerous environmental phenomena like in the convection in the outer core (Christensen et al. 1999) and in the ocean (Marschall and Scott 1999; Kamphuis et al. 2011) or in numerous atmospheric processes (Dickey et al. 1990).

✉ Tamás Bozóki
bozoki.tamas93@gmail.com

[1] Department of Geophysics and Space Science, Eötvös Loránd University, Pázmány Péter sétány 1/C, Budapest 1117, Hungary

Since the motion governed by rotation is often initiated by thermal inhomogeneities, the rotation influenced Rayleigh–Bénard convection has been in the focus of many scientific investigations (e.g., Scheel 2007; Zhong et al. 2009). In Earth's mantle the fictitious forces which appear due to rotation, namely the Coriolis- and the centrifugal force are commonly accepted to be negligible (Schubert et al. 2001) and are not taken into account in the most numerical simulations. However the demand for more and more precise numerical models to explain recent observations generates the need for the refined investigation of the effect of Earth's rotation on mantle convection.

The existence of negative shear wave anomalies in the lowest mantle beneath Africa and Pacific was revealed by seismic tomography (Garnero et al. 2007; Lay et al. 2004). They are called large low shear velocity provinces (LLSVP) owing to the decrease in shear wave velocity by 2–4 % but the relative indifference in pressure wave (0–2 % decrease). On the other hand it brings on henceforward numerous unanswered questions, mostly about its evolution and long-lived stability (Dziewonski et al. 2010). It is supposed to be compositionally denser by 2–4 % due to the increased iron content compared to the overlying part of the lower mantle (Tackley 2012), which can be explained by its chemical reaction with the core (Mao et al. 2006) or the crystallisation and differentiation of the mantle in the early Earth history (Labrosse et al. 2007). LLSVP reaches 800–1000 km height from the core-mantle boundary (Garnero and McNamara 2008) and its equatorial, nearly antipodal position beneath Africa and Pacific raises the possibility that its existence and position is correlated with the Earth's rotation. The surface hotspots are likely to be situated over the edge of these seismically slow provinces (Thorne et al. 2004) not only in the present but, by taking into account the plate tectonic movements, at least during the last 200 m years too (Torsvik et al. 2010). Indeed Dziewonski et al. (2010) showed that in the last 200 Myr the rotational axes of the Earth always changed along the meridian which separates the two, presumably denser provinces, hereby the maximal moment of inertia was always ensured. These two statements, the situation of hotspots and the changing of rotational axes presume that the nearly antipodal anomalies over the core-mantle boundary are stable formations of the mantle, they might have been existent and in this way have stabilised the whole rotating system since the early differentiation of Earth's internal structure.

It is well known that besides the angle of the rotation its magnitude changes also during the history of the Earth (Glukhovskii and Kuz'min 2015). The Earth's angular velocity decreased mostly because of tidal friction thus it is directly connected to the Earth–Moon distance which determines the intensity of tidal motion. It is presumed that the Earth's collision with a cosmic body, whose weight was similar to that of Mars, generated the Moon (Canup and Asphaug 2001; Harrison 2006; Wood 2011). After the collision the Earth–Moon distance was approximately 20 times less than it is today (Binder 1982; Bott 1982; Hazen 2012), which can be directly converted into the length of the day, which could be between 2 and 6 h (Glukhovskii and Kuz'min 2015). Hereby, the effect of rotation could be much more significant in the past, than it is today. Other hypothesis set this value to 8 h (Marakushev et al. Marakushev et al. 2013), which is three times less compared to the present value by all means. One of the few geological evidences of angular velocity in the past was presented by Erikson and Simpson (2000), who investigated the earliest sediments preserving the tidal stratification. He presumed that 3.2 b years ago the length of the day was closer to 15 than to 24 h. It is also possible to combine angular velocity data derived from fossils and tidal deposits with determinable lunar tidal torque values to estimate the angular velocity of the Earth through the last 4.55 Myr (Varga 2006; Varga et al. 1998). This method is the reverse approach of the problem and gives much less

changing in the length of the day, which could be between 15 and 20 h in the Katarchean (3.00–4.55 Ga). Thus this method gives much less change in the Earth–Moon distance too.

The considerable variation in the magnitude of Earth's rotation demands to reconsider whether it had contributed significantly to the evolution of the present-day Earth's mantle structure. In this study we investigate the possible deformation of the chemical inhomogeneities in the lowest mantle caused by Earth's rotation without thermal convection. We determine what magnitude of the deformation could be maintained by the rotation and what magnitude of rotation would be needed to generate domes with height similar to that of LLSVP.

2 Theoretical background and model description

The problem of the deformation of two non-miscible, isothermal fluids with different density can be handled by the continuity (1), the Navier–Stokes (2) and the mass transport Eq. (3),

$$\frac{\partial \rho}{\partial t} + \frac{\partial}{\partial x_i}(\rho \cdot u_i) = 0, \tag{1}$$

$$\rho\left(\frac{\partial u_i}{\partial t} + u_k \frac{\partial u_i}{\partial x_k}\right) = -2\,\rho\,\varepsilon_{ijk}\Omega_j u_k + \rho\left[g e_i - \left(\Omega_i\Omega_k - \Omega^2\delta_{ik}\right)x_k\right] - \frac{\partial p}{\partial x_i} + \frac{\partial \sigma_{ij}}{\partial x_j}, \tag{2}$$

$$\frac{\partial c}{\partial t} + u_i \frac{\partial c}{\partial x_i} = \frac{\partial}{\partial x_i}\left(D\frac{\partial c}{\partial x_i}\right). \tag{3}$$

Physical parameters used in the article are summarized in Table 1. The equations ensure the conservation of mass (1), the momentum (2) and the amount of the dense component (3) in the system. The impact of Earth's rotation appears in the Navier–Stokes equation,

Table 1 Symbol descriptions and dimensions

Symbol	Description	Dimension
ρ	Density	kg/m^3
t	Model time	s
u_i	Velocity field components	m/s
x_i	Space coordinates	m
ε_{ijk}	Levi–Civita symbol	1
Ω_i	Earth's angular velocity	1/s
g	Gravitational acceleration	m/s^2
e_i	Unit vector, pointing downwards	1
δ_{ik}	Kronecker delta	1
p	Pressure	Pa
σ_{ij}	Deviatoric stress tensor	Pa
c	Normalised concentration of the dense material	1
D	Diffusion coefficient	m^2/s
β	Relative density difference between the lowermost and the overlaying mantle	1
ρ_d	Density of the dense material	kg/m^3

where the momentum of the fluid (left side) is affected by the Coriolis force, gravitational force, centrifugal force, the pressure gradient and the viscous force in the right side of Eq. (2).

Boussinesq approximation (Chandrasekhar 1961) can be used to simplify the equation system and the mantle can be handled as a fluid with Newtonian rheology. According to Boussinesq approximation the gravitational acceleration (g), the dynamic viscosity (η) and the diffusion coefficient (D) are fixed to constant, average values are representative to the Earth's mantle similarly to the density (ρ) which is constant except within the term describing the chemical buoyancy force. The normalized concentration shows the dense matter content of the fluid,

$$c = \frac{\rho - \rho_0}{\rho_d - \rho_0}, \tag{4}$$

thus $c = 1$ represents the dense and $c = 0$ the light component of the mantle. In isothermal mantle the generally temperature dependent equation of state becomes simplified,

$$\rho = \rho_0 \cdot (1 + \beta \cdot c), \tag{5}$$

where β denotes the relative density difference between the two mantle components,

$$\beta = \frac{\rho_d - \rho_0}{\rho_0}. \tag{6}$$

The equation system (1), (2), (3) take the following form after the approximation described above:

$$\frac{\partial u_i}{\partial x_i} = 0, \tag{7}$$

$$\rho_0 \left(\frac{\partial u_i}{\partial t} + u_k \frac{\partial u_i}{\partial x_k} \right) = -2\, \rho_0\, \varepsilon_{ijk}\, \Omega_j\, u_k + \rho(c) \cdot \left[g \cdot e_i + (\Omega_i \cdot \Omega_k - \Omega^2 \cdot \delta_{ik})\, x_k \right] - \frac{\partial p}{\partial x_i} + \eta \frac{\partial^2 u_i}{\partial x_j^2}, \tag{8}$$

$$\frac{\partial c}{\partial t} + u_i \frac{\partial c}{\partial x_i} = D \frac{\partial^2 c}{\partial x_i^2}. \tag{9}$$

By separating the hydrostatic and the dynamic pressure (δp) in Navier–Stokes Eq. (8) the constant term of density and hydrostatic pressure will be cancelled,

$$\rho_0 \frac{du_i}{dt} = -2\, \rho_0\, \varepsilon_{ijk}\, \Omega_j\, u_k + \rho_0\, \beta\, c \left[g \cdot e_i + (\Omega_i \cdot \Omega_k - \Omega^2 \cdot \delta_{ik})\, x_k \right] - \frac{\partial \delta p}{\partial x_i} + \eta \frac{\partial^2 u_i}{\partial x_j^2}. \tag{10}$$

In order to determine whether the centrifugal force and/or the Coriolis force could play an important role in the mantle flow dimensional analysis must be applied (Schubert et al. 2001). The dimensionless Navier–Stokes equation takes the following form:

$$\frac{1}{\mathrm{Pr}} \frac{du_i}{dt} = -\frac{2}{Ek} \varepsilon_{ijk}\, \Omega_j\, u_k + Ra_C\, c\, e_i + Ra_{CR}\, c \left(\Omega_i \cdot \Omega_k - \Omega^2 \cdot \delta_{ik} \right) x_k - \frac{\partial \delta p}{\partial x_i} + \frac{\partial^2 u_i}{\partial x_j^2}, \tag{11}$$

where Pr, Ek, $\mathrm{Ra_C}$ stands for the Prandtl, the Ekman and the compositional Rayleigh number, respectively. Table 2 contains the average values of these dimensionless numbers

Table 2 Model constants

Description	Symbol	Value
Gravitational acceleration	g	10 m/s^2
Dynamic viscosity	η	10^{22} Pa s
Diffusion coefficient	D	10^{-11} m^2/s
Earth's angular velocity	Ω_0	7.29^{-5} 1/s
Earth radius	R_0	6370 km
Core radius	R_1	3470 km
Bulk density	ρ_0	4500 kg/m^3
Thermal diffusivity	κ	10^{-6} m^2/s

for the mantle. Taking into account the role of the centrifugal force, a new non-dimensional parameter was defined. Ra_{CR} denotes the ratio of the centrifugal force in the compositionally non-homogeneous mantle and the viscous force,

$$Ra_{CR} = \frac{\rho_0 \beta \, \Omega_0^2 d^4}{\eta_0 \kappa} \cong 5 \cdot 10^3. \tag{12}$$

The value of Ra_{CR} is estimated based on the present-day mantle parameters.

Based on the value of the Prandtl and Ekman number the influence of the inertia and Coriolis-force can be excluded unequivocally, thus Eq. (11) can be simplified,

$$0 = Ra_C \; c \; e_i + Ra_{CR} \; c \; \left(\Omega_i \cdot \Omega_k - \Omega^2 \cdot \delta_{ik}\right) \; x_k - \frac{\partial \delta p}{\partial x_i} + \frac{\partial^2 u_i}{\partial x_j^2}. \tag{13}$$

At the same time the value of the dimensionless number related to the centrifugal force imply that it might influence the convection. Compare the value Ra_{CR} with Ra_C and Ra_T (Table 3), which govern the thermo-chemical convection in the mantle, 3–4 order of magnitude is the difference, however taking into account the angular velocities possible in the Earth's history, the difference decrease appreciably (Table 4). Consequently the dimensionless equation does not justify the neglection of centrifugal force and hereby the effect of Earth's rotation on mantle convection.

Another important property of the centrifugal force is that it breaks the spherical symmetry in the convection, by assigning a particular, equatorial direction. Furthermore, contrary to the Coriolis force, centrifugal force is not attached to movements thus it is able to generate and stabilise equilibrium deformations (like the shape of Earth). Due to this property it can directly affect the boundary conditions of the thermo-chemical convection in the mantle. While it has an obvious impact on the surface, its effect on the global geodynamics has yet to be clarified.

Two-dimensional cylindrical shell geometry has been applied to study the effect of the centrifugal force on the compositionally heterogeneous mantle without thermal convection. Rotation axis lies in the 2D plain and points to the imaginary north–south direction, thus the model can be interpreted as a vertical section of a planet. COMSOL Multiphysics 4.2a finite element numerical modelling software was used to solve equations of (7), (9) and dimensional Navier–Stokes Eq. (14) derived from Eq. (13),

$$0 = \rho_0 \; \beta \; c \; \left[g \cdot e_i + \left(\Omega_i \cdot \Omega_k - \Omega^2 \cdot \delta_{ik}\right) \; x_k\right] - \frac{\partial \delta p}{\partial x_i} + \eta \frac{\partial^2 u_i}{\partial x_j^2}. \tag{14}$$

Table 3 Dimensionless numbers and their characteristic values for the mantle (Schubert et al. 2001)

Symbol	Dimensionless number	Average value for the mantle
Pr	Prandtl number	10^{23}
Ek	Ekman number	10^{9}
Ra_C	Compositional Rayleigh number	10^{6}
Ra_T	Thermal Rayleigh number	10^{6}–10^{7}

Table 4 Values of Ra_{CR} at different angular velocity magnitude and length of day (T) possible in Earth's history

Ω/Ω_0	T (h)t in xm;	Ra_{CR}
1	24	5×10^3
3	8	5×10^4
4	6	8×10^4
12	2	7×10^5

Boundaries were stress-free and impermeable for mass transport. The surface and the core–mantle boundary were fixed during the simulation in order to concentrate on the inner mantle deformation. As an initial condition a dense layer with a thickness of 300 km encircles the core (Fig. 1a) which fits the shape of LLSVPs and explains the location of hotspots best (Li et al. 2014). Deformation height of the dense layer was characterized by the elevation parameter δh (measured from the surface of the initial dense layer), which was defined by the concentration value of $c = 0.5$. We investigated the equatorial elevation that is the maximum deformation in this study (Fig. 1b).

The model domain was discretized by triangular finite elements. Two types of grid had been used, one with finer mesh for the whole mantle (grid 1, Fig. 2a) and one with finer mesh at the initial boundary between the two layers (grid 2, Fig. 2b). In grid 1 the maximum element size for the whole mantle was 75 km and at the surface of the dense layer 2 km with a total element number of 396,790, while in grid 2 these values were 200 km, 1 km and 689,506, respectively. In this way grid 2 was more appropriate to investigate small deformations of the lower dense layer.

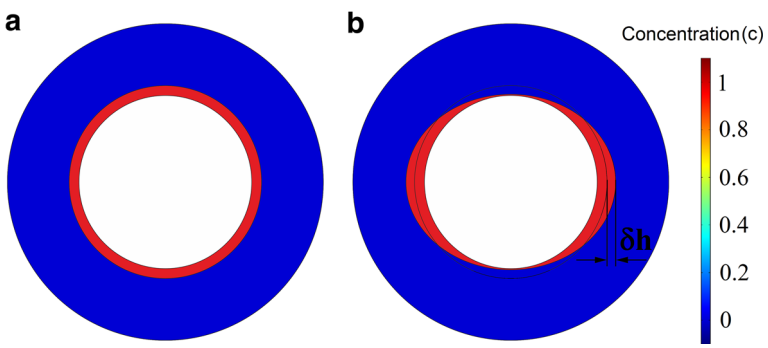

Fig. 1 **a** Initial concentration distribution of the dense layer as well as **b** the sketch of the deformation and the definition of the elevation parameter, δh

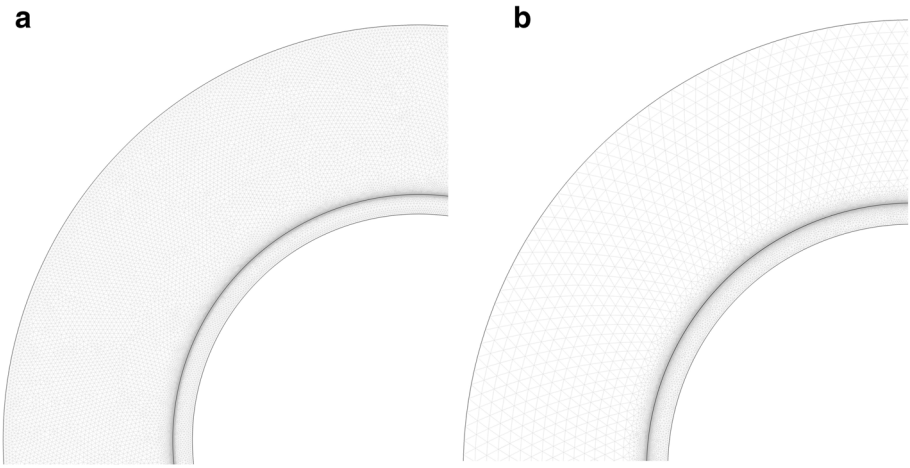

Fig. 2 Finite element mesh **a** grid 1 and **b** grid 2 used in simulations

3 Model results

Figure 3 illustrates the elevation parameter, δh as a function of time at different compositionally density difference between the layers, β. First, the angular velocity of the Earth was constant (Ω_0), while β varied from 1 to 10 % as a consequence of the uncertainty in the compositional density difference in the lowermost mantle. In this way Ra_{CR} changes between 1.7×10^3 and 1.7×10^4 in different simulations. Based on the results obtained from seismic tomography, thermo-chemical model calculations and normal modes of the Earth (Koelemeijer et al. 2012; Ishii and Tromp 2004; Tackley 2012; Galsa et al. 2015) β = 2–4 % might be a reasonable value for the LLSVP.

The evolution of the equatorial surface elevation shows an exponentional relaxation to an equilibrium state in every case. Elevation parameter values were calculated at each 10 Myr, and a function of

$$\delta h = A_\beta + B_\beta \exp\left(-\frac{t}{\tau_\beta}\right) \tag{15}$$

was fitted on the numerical data. Table 5 contains all fitted parameter in this study. The quality of fitting was high ($\chi^2 > 0.999$ for each curve), after the time of 5τ the deformation reached the 99 % of the equilibrium. It was established, that the equilibrium elevation height does not depend on the relative density difference, β, the equatorial, equilibrium elevation height was found to be approximately $A_\beta = 2$ km in every model (Fig. 3).

Figure 4 shows the fitted relaxation time constant, τ_β as a function of the relative density difference. The plot was fitted using a function of

$$\tau_\beta = \frac{C}{\beta}; \tag{16}$$

consequently τ_β is proportional to the reciprocal of density difference between the layers. This result shows considerably similarity to the well-known viscous relaxation problem as the post glacial rebound (Haskell 1935), where the explicit value of the relaxation time

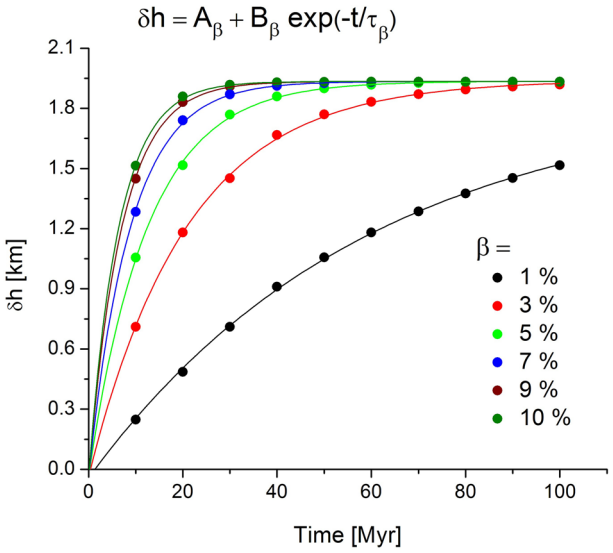

Fig. 3 Elevation parameter as a function of time at different relative density differences between the layers (β). Exponential function described in Eq. (15) was fitted on numerical data

depends on the viscosity (η) and the density (ρ) of the mantle as well as the wave length of the initial depression (λ),

$$\tau = \frac{4\pi\eta}{\rho g \lambda}. \tag{17}$$

In the range of $\beta = 2$–4 % the time constant is approximately 30–15 Myr, which is a relative short period compared to Earth history, but much longer than that of the post-glacial rebound (circ. 2000–5000 year (Schubert et al. 2001)).

Since the angular velocity of the planet has varied owing to the tidal dissipation the effect of Ω was investigated as well. Figure 5 represents the evolution of the elevation height at different relative angular velocities (Ω/Ω_0), while the relative compositional density difference was held at a realistic constant rate of $\beta = 3$ %. Ra_{CR} changes between 5×10^3 ($\Omega = \Omega_0$) and 5×10^5 ($\Omega = 10 \times \Omega_0$) in different simulations. The time variation of the elevation parameter reflects a similar trend to the effect of β (Fig. 3), thus an exponential relation was fitted on data obtained from numerical models at each 10 Myr with A_Ω, B_Ω and τ_Ω fitted parameters (Table 5). Obviously, higher angular velocity results in larger equatorial deformation.

The equilibrium deformation as a function of the relative angular velocity shows power law dependence (Fig. 6a), where the fitted

$$A_\Omega = D \cdot (\Omega/\Omega_0)^E \tag{18}$$

function's exponent is roughly equal to two, namely $E = 2.135 \pm 0.01$. We note, the value of $E = 2$ gives the centrifugal force for an individual mass point. However, Fig. 6b displays that τ_Ω is independent of the angular velocity. The deformation reaches the magnitude of 100 km at about $\Omega/\Omega_0 = 7$, the total thickness of the actual LLSVP only at

Table 5 Fitted parameters of Eq. (15), (16) and (18)

	β					
	1	3	5	7	9	10
A_β (km)	1.88 ± 0.03	1.94 ± 0.01	1.934 ± 0.004	1.934 ± 0.002	1.934 ± 0.002	1.934 ± 0.002
B_β (km)	−1.92 ± 0.02	−1.97 ± 0.01	−1.97 ± 0.01	−1.97 ± 0.01	−1.97 ± 0.01	−1.96 ± 0.01
τ_β (Myr)	59 ± 2	21.0 ± 0.3	12.5 ± 0.1	8.9 ± 0.1	7.07 ± 0.06	6.42 ± 0.05
	Ω/Ω_0					
	1	2	3	4	5	6
A_Ω (km)	1.906 ± 0.002	7.67 ± 0.01	17.13 ± 0.01	30.62 ± 0.03	48.7 ± 0.1	70.8 ± 0.2
B_Ω (km)	−1.89 ± 0.003	−7.69 ± 0.02	−17.04 ± 0.02	−30.65 ± 0.06	48.7 ± 0.2	−70.8 ± 0.3
τ_Ω (Myr)	20.6 ± 0.1	20.3 ± 0.2	19.97 ± 0.06	19.7 ± 0.1	19.8 ± 0.2	19.7 ± 0.2
	Ω/Ω_0					
	7	8	9	10		
A_Ω (km)	99.3 ± 0.2	132.7 ± 0.3	171.0 ± 0.7	213.5 ± 0.9		
B_Ω (km)	−99.3 ± 0.4	−133.0 ± 0.5	−170.8 ± 1.2	−213.7 ± 1.6		
τ_Ω (Myr)	19.9 ± 0.2	19.8 ± 0.2	19.7 ± 0.3	19.1 ± 0.3		
C (Myr)	0.602 ± 0.005					
D (km)	1.564 ± 0.03					
E (1)	2.135 ± 0.01					

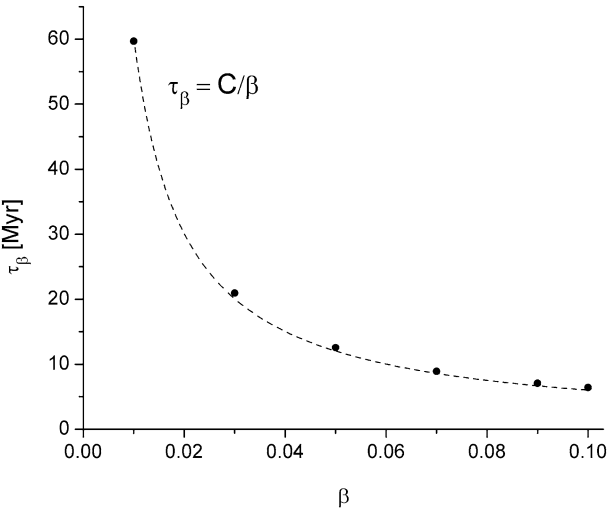

Fig. 4 Relaxation time of deformation as a function of β. Reciprocal function (Eq. 16) was fitted on data

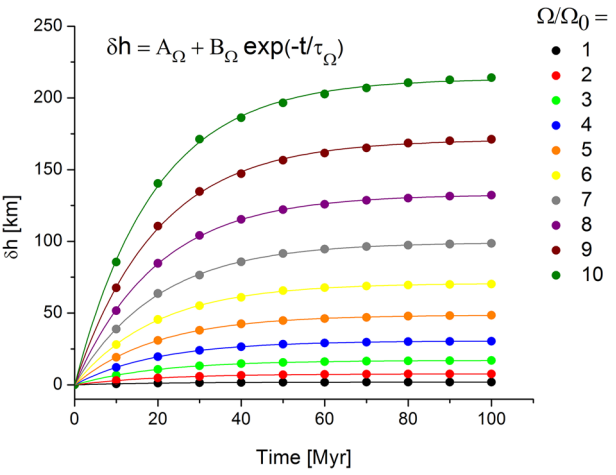

Fig. 5 Elevation parameter as a function of time at different relative angular velocity values

approximately 15, where the total thickness is measured from the core-mantle boundary obviously.

The root-mean-square velocity of the flow system depends on both the relative density difference and the angular velocity (Fig. 7). Being in accordance with Fig. 3 higher β results in faster initial deformation and larger slope of velocity decrease, so smaller τ_β (Fig. 7a). On the other hand, faster deformation occurs at higher rotation (Fig. 7b), however, velocity curves do not intersect indicating the constant relaxation time. Summarized, the elevation height is independent of the density difference but depends on the angular velocity, while the relaxation time characterizing the time till the equilibrium of the deformation depends on the density contrast but is independent of the angular velocity.

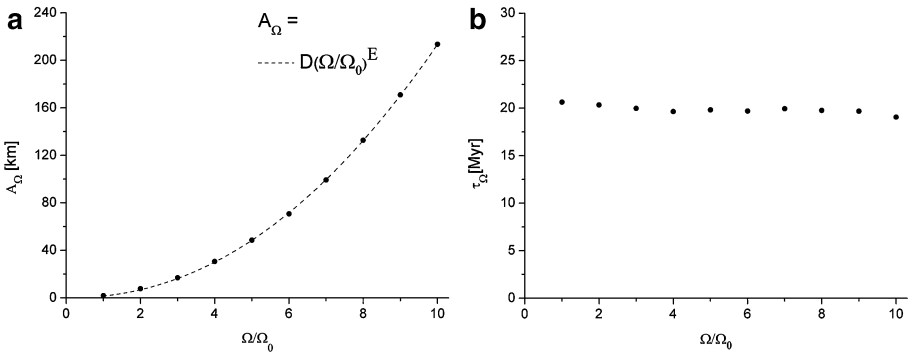

Fig. 6 **a** The equatorial equilibrium elevation height and **b** the relaxation time of the deformation as a function of the relative angular velocity. Power function described by Eq. (18) was used for fitting

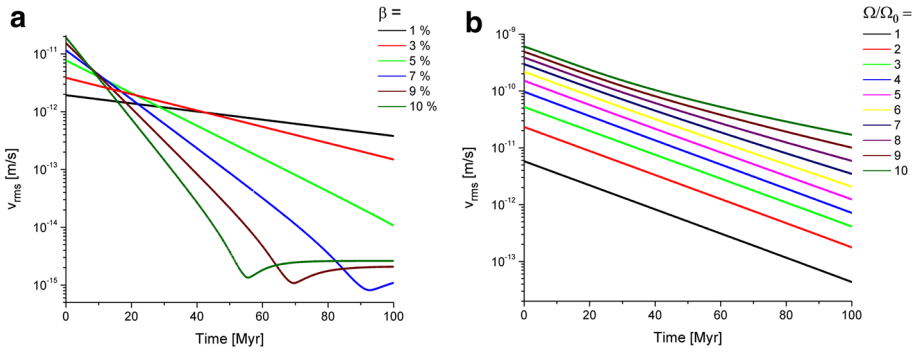

Fig. 7 Time-variation of root-mean-square velocity (v_{rms}) **a** at different β and **b** Ω/Ω_0 values

4 Discussion and conclusions

The main aim of the study was to investigate the influence of the centrifugal force due to the Earth's rotation on the evolution of the compositionally dense layer in the lowermost mantle. A new non-dimensional parameter, Ra_{CR} was defined to quantify the centrifugal force related to the viscous force. Dimensional analysis pointed out that the role of the centrifugal force is not obviously negligible for the Earth's mantle contrary to the inertia and Coriolis force. In Earth's history the centrifugal force could be commensurable with the thermal (Ra_T) and compositional (Ra_C) buoyancy force, which generate the thermo-chemical convection in the mantle. The dimensionless equations, the apparent impact on the shape of Earth, the property of being independent of motion contrary to Coriolis force together motivated the importance of investigation of the centrifugal force. It is obvious that the centrifugal force breaks the spherical symmetry in the mantle flow. Question is whether it is able to induce a significant deformation of the lower mantle density inhomogeneities or it only appoints the stable, equilibrium direction with maximal moment of inertia.

According to the simulations the rotation does not generate dense domes with remarkable heights at Earth's angular velocity. At faster rotation possible in the Earth's

history the height of the deformation might have been reached the magnitude of 380–400 km. Although this deformation is half/third of the actual height of LLSVP, palpable asymmetry appears in the mantle. It is possible that this asymmetry can be thickened by other phenomena (e.g., subducted slabs at the core mantle boundary). Another important result toward the complex simulations can be the independence of elevation height of the relative density difference between the two layers. The relaxation time constant of some 10 Myr is not certainly exact however it can imply that the built up of deformation needs relatively short time at geological time scale.

The stabilization effect of the centrifugal force was not investigated in this study however it can be one of the most important property of the rotation. As it was mentioned above the LLSVP seems to be stable formations of the lower mantle, the survival of these phenomena could be facilitated by also the centrifugal force. Probably a compositionally dense dome evolved in arbitrary direction would have been forced into equatorial direction by the centrifugal force.

This study may reveal that it is important to investigate the influence of centrifugal force in the mantle. At least two types of models could provide important information. First question is whether the small asymmetry caused by centrifugal force in the lower mantle toward an appointed direction can be strengthened by other effects in thermo-chemical mantle convection. The second model should investigate the stabilization effect of the centrifugal force in thermo-chemical convections. If dense material accumulation appears somewhere in the lower mantle near the core-mantle boundary, how could the centrifugal force constrain it into equatorial position. Thus, the centrifugal force could be able to affect the convection in the mantle.

Acknowledgments This research was supported by the European Union and the State of Hungary, co-financed by the European Social Fund in the framework of TÁMOP 4.2.4. A/1-11-1-2012-0001 National Excellence Program and by the Hungarian Science Foundation under Grant number NK100296.

References

Binder AB (1982) The Moon: its figure and orbital evolution. Geophys Res Lett 9(1):33–36

Bott MHP (1982) The interior of the earth: its structure, constitution and evolution, 2nd edn. Elsevier, London

Canup RM, Asphaug E (2001) Origin of the Moon in a giant impact near the end of the Earth's formation. Nature 412(6848):708–712

Chandrasekhar S (1961) Hydrodynamic and hydromagnetic stability. Clarendon, Oxford

Christensen U, Olson P, Glatzmaier GA (1999) Numerical modelling of the geodynamo: a systematic parameter study. Geophys J Int 138(2):393–409

Dickey JO, Ghil M, Marcus SL (1990) A 30–60 day oscillation in length-of-day and atmospheric angular momentum: extratropical origin? In: Boucher C, Wilkins GA (eds) Earth rotation and coordinate reference frames. Springer, New York, pp 90–97

Dziewonski AM, Lekic V, Romanovicz BA (2010) Mantle anchor structure: an argument for bottom up tectonics. Earth Planet Sci Lett 299(1–2):69–79

Eriksson KA, Simpson EL (2000) Quantifying the oldest tidal record: the 3.2 Ga Moodies Group, Barberton greenstone belt, South Africa. Geology 28(9):831–834

Galsa A, Herein M, Lenkey L, Farkas MP, Taller G (2015) Effective buoyancy ratio: a new parameter characterizing thermo-chemical mixing in the Earth's mantle. Solid Earth 6:93–102

Garnero E, McNamara A (2008) Structure and dynamics of Earth's lower mantle. Science 320(5876):626–628

Garnero EJ, Lay T, McNamara A (2007) Implication of lower-mantle structural heterogeneity for existence and nature of whole-mantle plumes. Geol Soc Am Spec Pap 430:79–101

Glukhovskii MZ, Kuz'min MI (2015) Extraterrestrial factors and their role in the Earth's tectonic evolution in the early Precambrian. Russ Geol Geophys 56(15):959–977
Harrison TM (2006) Exploring the hadean earth. Geochim Cosmochim Acta 70(18S):A234
Haskell NA (1935) The motion of a fluid under the surface load. Physics 6:265–269
Hazen R (2012) The story of earth: the first 4.5 b years, from stardust to living planet. Viking, New York
Ishii M, Tromp J (2004) Constraining large-scale mantle heterogeneity using mantle and inner-core sensitive normal modes. Phys Earth Planet Inter 146(1–2):113–124
Kamphuis V, Huisman SE, Dijkstra HA (2011) The global ocean circulation on a retrograde rotating earth. Clim Past 7(2):487–499
Koelemeijer PJ, Deuss A, Trampert J (2012) Normal mode sensitivity to Earth's D'' layer and topography on the core-mantle boundary: what we can and cannot see. Geophys J Int 190(1):553–568
Labrosse S, Hernlund JW, Coltice N (2007) A crystallizing dense magma ocean at the base of Earth's mantle. Nature 450(7171):866–869
Lay T, Garnero EJ, Williams Q (2004) Partial melting in a thermo-chemical boundary layer at the base of the mantle. Phys Earth Planet Inter 146(3–4):441–467
Li Y, Dechamps F, Tackley PJ (2014) The stability and structure of primordial reservoirs in the lower mantle: insights from models of thermochemical convection in three-dimensional spherical geometry. Geophys J Int 199:914–930
Mao WL, Shu JF, Hu JZ, Hemley R, Mao H (2002) Displacive transition in magnesiowüstite. J Phys-Condens Matter 14(44):11349–11354
Marakushev AA, Zinov'eva NG, Paneyakh NA, Marakushev SA (2013) The origin and evolution of the solar system. Prostran i Vremya 2(12):132–141
Marschall J, Scott F (1999) Open-ocean convection: observations, theory, and models. Rev Geophys 37(1):1–64
Scheel J (2007) Rotating rayleig-bénard convection. Dissertation, California Institute of Technology
Schubert G, Turcotte D, Olson P (2001) Mantle convection in the earth and planets. University Press, Cambridge
Tackley PJ (2012) Dynamics and evolution of the deep mantle resulting from thermal, chemical, phase and melting effects. Earth Sci Rev 110(1–4):1–25
Thorne MS, Garnero EJ, Grand S (2004) Geographic correlation between hot spots and deep mantle lateral shear-wave velocity gradients. Phys Earth Planet Inter 146(1–2):47–63
Torsvik TH, Steinberger B, Gurnis M, Gaina C (2010) Plate tectonics and net lithosphere rotation over the past 150 My. Earth Planet Sci Lett 291(1–4):106–112
Varga P (2006) Temporal variation of geodynamical properties due to tidal friction. J Geodyn 41(1–3):140–146
Varga P, Denis C, Varga T (1998) Tidal friction and its consequences in paleogeodesy, in the gravity field variations and in tectonics. J Geodyn 25(1):61–84
Wood B (2011) The formation and differentiation of Earth. Phys Today 64(12):40–45
Zhong J Q, Stevens R, Clercx H, Verzicco R, Lohse D, Ahlers G (2009) Prandtl-, Rayleigh-, and Rossby-number dependence of heat transport in turbulent rotating Rayleigh–Bénard convection. Physical Review Letters 102(4):044502